An Efficient CT Image Reconstruction with Parallel Modeling for Superior Quantitative Measures

S.Asif Hussain[1]
Associate professor
Department of ECE, A.I.T.S,
Rajampet, Andhra Pradesh, India
e-mail: sah.ssk@gmail.com

K. Lokeswara Reddy[2]
M.Tech (E.S) student
Department of ECE,
A.I.T.S Rajampet, A.P, India
e -mail: lokes9@gmail.com

ABSTRACT

Image segmentation algorithms based on ROI typically rely on the homogeneity of image intensities. CT scanner is dedicated as research Scanner which has been developed in view of imaging applications. A key Feature of the work is to use Empirical system to achieve resolution recovery with novel region based method. This method identifies local intensity cluster with local clustering criterion function with respect to neighborhood center. Reconstruction quality is analyzed quantitatively in terms bias field correction for intensity inhomogenity correction. This method is valid on synthetic images of various imaging modalities. A significant improvement in reconstruction quality can be realized by faster and more accurate visual quality quantitative measures where Reconstruction quality is analyzed quantitatively in terms of bias-variance measures (bar phantom) and mean square error (lesion phantom). However, with the inclusion of the empirical kernel, the iterative algorithms provide superior reconstructions compared to FBP, both in terms of visual quality and quantitative measures. Simulated results show improved tumor bias and variance characteristics with the proposed algorithm.

Keywords: Intensity inhomogeneities, Empirical system kernel, Bias-variance, Iterative algorithms

1. INTRODUCTION

Image segmentation is often an essential step before further image-processing of three-dimensional medical images canbe done. An object can be segmented based on shape and/or intensity characteristics. The task of image segmentation can be simplified with initialized parameters to guide accurate segmentation. Semi-automated and interactive methods [1] have been relatively successful, but require varying degrees of human input. Segmentation is often an important step in US B-mode image analysis .we consider the problem of correcting for attenuation-related intensity inhomogenieties i.e., those that cause a slowly changing (low-frequency) intensity contrast and are not due to speckle-mode imaging artifacts include speckle noise, attenuation(absorption and scattering), etc. The statistical analysis and reduction of speckle noise has been studied extensively in the literature [1]–[7]. Other artifacts, particularly those caused by non uniform beam attenuation within the body that are not accounted for by *time gain compensation* (TGC), also decrease the image signal-to-noise ratio (SNR).Existing level set methods for image segmentation can be categorized into two major classes: *region-based models* [4], [10], and *edge-based models* [3], [7], [8], [12]. Region-based models aim to identify each region of interest by using a certain region descriptor to guide the motion of the active contour. However, it is very difficult to define a region descriptor for images with intensity inhomogeneities. Most of region-based models [4], [16] are based on the assumption of intensity homogeneity. Edge-based models use edge information for image segmentation. These models do not assume homogeneity of image intensities, and thus can be applied to images with intensity inhomogeneities. A novel region-based method for image segmentation. From a generally accepted model of images with intensity inhomogeneities, we derive a local intensity clustering property, and therefore define a local clustering criterion function for the intensities in a neighbourhood of each point. This local clustering criterion is integrated over the neighbourhood center to define an energy functional, which is converted to a level set formulation. Minimization of this energy is achieved by an interleaved process of level set evolution and estimation of the bias field. As an important application, our method can be used for segmentation and bias correction of magnetic resonance(MR) images.

2. Methods:

BACKGROUND:

In this section, we review the method proposed by Zhang for estimating the field B_1 distortion and simultaneously segmenting an MR image and provide implementation details on how it has been adapted to work with US images. This method essentially estimates the low (spatial)-frequency multiplicative degradation field while at the same time identifying regions of similar intensity inhomogeneity using an MRF-MAP frame work. As we will explain in Section III, although developed for another imaging modality, under simplified assumptions, we can justify using the same approach on displayed US images.

2.1 Model Specification:

Let S be a lattice indexing the pixels in the given image. Further,

$$I = (I_{1,\dots}I_{N)} \text{ and } I^{*} = (I_1^{*}, \dots, I_N^{*})$$

let and be the observed and the ideal (that is, without intensity inhomogeneity distortion) intensities of the given image respectively, being the number of pixels in the image. We assume that the distortion at pixel $1 \leq i \leq N$ can be expressed by a multiplicative model of the form

$$I_{i=}I_i^{*} \times d_i \qquad (1)$$

Where$d_i$represents the gain of the intensity due to the intensity inhomogeneity at pixel . A logarithmic transformation of this equation yields an addition. Let $y$andy^{*}denote, respectively ,the observed and the ideal log-transformed intensities, then

$$y = y^* + d \qquad (2)$$

Where d denotes the log-transformed intensity distortion field. Segmentation can be considered as a problem of statistical classification, which is to assign every pixel a class label from a label set. Let L denote the label set. A labeling of S will be denoted by X, in which $x_i x_i \in L$ is the corresponding class label of pixel i.Given the class label x_i , it is assumed that the intensity value at pixel i, y_i^* follows a Gaussian distribution(this assumption will be justified in Section III) with parameter $\theta(x_i) = (\mu_{xi}, \sigma_{xi}), \mu_{xi}, \sigma_{xi}$ being the mean and the variance of class x_i, respectively

$$p(y_i^*|x_i) = g(y_i^*; \theta(x_i)) \qquad (3)$$

where

$$g(y;\theta) = {}^{1}/_{\sqrt{2\pi\sigma^2}} \exp\left(-\frac{(y-\mu)^2)}{2\sigma^2}\right).$$

With the distortion field taken into account, the above distribution can be written in terms of the observed intensity y_i as

$$p(y_i|x_i, d_i) = g(y_i - d_i; \theta(x_i)) \qquad (4)$$

and, hence, a class-independent intensity distribution

$$p(y_i|d_i) = \sum_{j\in L}\{g(y_i - d_i; \theta(x_i))p(x_i = j)\} \qquad (5)$$

Thus, the intensity distribution at pixel i is modeled as a Gaussian mixture, given the distortion field. Assuming that the pixel intensities are statistically independent, the probability density for the entire image, given the distortion field, is

$$p(y|d) = \prod_{i\in s} p(y_i|d_i), \qquad (6)$$

Bayes' rule can be used to obtain the posterior probability of the distortion field, given the observed intensity values

$$p(d|y) = \frac{p(y|d)p(d)}{p(y)} \qquad (7)$$

Where $p(y)$ is a normalization constant. The prior probability density of the distortion field $p(d)$ is modeled as a Gaussian with zero mean to capture its smoothness property. The maximum *a posteriori* (MAP) principle can be employed to obtain the optimal estimate of the distortion field $\hat{d}$, given the observed intensity values

$$\hat{d} = arg\max_d p(d|y). \qquad (8)$$

The optimum solution $\hat{d}$ satisfies the following condition

$$\left[\frac{\partial}{\partial d_i} lnp(d|y)\right]_{d=\hat{d}} = 0 \quad \forall_i. \qquad (9)$$

Solving this equation leads to the update equations (see [12] for detail)

$$w_{ij} = \frac{p(y_i|x_i, d_i)p(x_i = j)}{p(y_i|d_i)} \qquad (10)$$

$$d_{i=}\frac{[FR]_i}{[F\psi^{-1}I]_i}, \text{ with I= } (1,1,\ldots,1)^T. \qquad (11)$$

Here, W_{ij} is the posterior probability that pixel i belongs to class j given the distortion field estimate, F is a low-pass filter, R is the *mean residual* in which for pixel i

$$R_i = \sum_{j\in L}\frac{w_{ij}(y_i - \mu_j)}{\sigma_j^2} \qquad (12)$$

And ψ is the *mean inverse covariance*, in which if otherwise.

$$\psi_{ik}^{-1} = \begin{cases}\sum_{j\in L} W_{ij}\sigma_j^{-2}, & if \ \ i = k \\ 0 & otherwise.\end{cases} \qquad (13)$$

2.2 Bayesian criterion for filtering edge information:

It is assumed that interpolated boundaries will partially overlap with the true edges found using edge detection. The probability of edges overlapping with shape-interpolated boundaries may be modeled using Bayes' probability. It is assumed that the probability of overlap at interpolated slices is greater than or equal to that at user-initialized contours. Edges are divided into edge components based on their connectivity. To retain edges with higher saliency, the edge components are sorted in descending order relative to the amount of overlap with the boundary. When the cumulative probability of overlap exceeds that obtained from user initialized contours, the remaining edge components are discarded. The Bayes' classification is thus not employed for training, but rather as a guide to how well boundaries can be defined based on edge detection.

3. Proposed Algorithms:

3.1 The 3-D Case:

The algorithm can be applied to 3-D volumes reconstructed from a sequence of parallel, closely spaced 2-D images. We assume that in such a sequence neighbouring slices resemble each other, that is, overlapping pixels in neighbouring slices tend to have the same class labels. Intensity in homogeneity field estimation is performed within each 2-D image, while the energy function in the MRF prior model involves a 3-D neighbourhood system, which includes, for each pixel in a 2-D scan, the eight nearest neighbours in the same scan and the two direct neighbours in the previous and the next scan. This 3-D constraint helps to strengthen ambiguous boundaries that are easily mislocated in2-D processing.

3.2 Boundary-edge correspondence:

Ideally, the match between boundary and edge should be one-to-one. However, deviations in the interpolated shape will not initialize *Bi* well. To prevent many-to-one snapping of boundary points, a minimum snapping-distance map is stored for every edge point. Subsequent boundary points will only be allowed to snap to the edge point if the snapping distance is less than or equal to the value in the minimum snapping-distance map. Therefore, boundary points will not arbitrarily snap to false edges if there are no edges to be found. During

the first iteration, the search window has not been adaptively altered to match the edge proximity for the image slice. There is a possibility that a false edge will be included in the Bayesian criterion. To prevent this, an inverse weighted distance transform, *M*, is multiplied to *Fi,k*, where *M* is a square matrix. Denoting *pq M* as an element in *M* and any two points on the *Bi* as *bp* and *bq*.,*pq M* is defined in Eq. 1.

$$M_{pq} = \frac{1}{\left\|b_p - b_q\right\| + 1} \qquad \ldots(1)$$

3.3 Local Intensity Clustering Property:

Region-based image segmentation methods typically relies on a specific region descriptor (e.g. intensity mean or a Gaussian distribution) of the intensities in each region to be segmented. However, it is difficult to give such a region descriptor for images with intensity inhomogeneities. Moreover, intensity inhomogeneities often lead to overlap between the distributions of the intensities in the regions$\Omega_1, \ldots, \Omega_N$. Therefore, it is impossible to segment these regions directly based on the pixel intensities .Nevertheless, the property of local intensities is simple ,which can be effectively exploited in the formulation of our method for image segmentation with simultaneous estimation of the bias field based on the image model in (3) and the assumptions A1and A2, we are able to derive a useful property of local intensities, which is referred to as a local intensity clustering property as described and justified below. To be specific, we consider a circular neighbourhood with a radius ρ centered at each point $y \in \Omega$ defined by $\varphi_y \triangleq \{x : |x-y| \leq \rho\}$. .The partition$\{\Omega_i N_{i=1}\}$of the entire domain Ω induces a partition of the neighbourhood $\varphi_y, i.e., \{\varphi_y \cap \Omega_i\} N_{i=1}$, i.e., forms a partition of φ_y. . For as lowly varying bias field$b$ the values$b(X)$ for all$X$in the circular Neighbourhood φ_y,are close to$b(y)$, i.e. for

$$b(X) \approx b(y) for X \in \varphi_y, \qquad (4)$$

Thus, the intensities $b(X)J(X)$in each sub region $\varphi_{y \cap \Omega_i}$ are close to the constant$b(y)C_i$ i.e.

$$b(X)J(X) \approx b(y)C_i \quad for \quad X \in \varphi_y \cap \Omega_i \qquad (5)$$

Then, in view of the image model in (3), we have

$$I(X) \approx b(y)C_i + n(X) \quad for \quad X \in \varphi_y \cap \Omega_i$$

Where $n(X)$is additive zero-mean Gaussian noise. Therefore, the intensities in the set

$$I_y^i = \{I(x) : x \in \varphi_y \cap \Omega_i\}$$

form a cluster with cluster center $m_i \approx b(y)C_i$, which can be considered as samples drawn from a Gaussian distribution with mean m_i . Obviously N, the clusters $I_y^1, \ldots, I_y^N$, are well-separated ,with distinct cluster centers $m_i \approx b(y)C_i, i = 1, \ldots, N$, (because the constants $C_1, \ldots, C_N$ are distinct and the variance of the Gaussian noise$n$ is assumed to be relatively small). This local intensity clustering property is used to formulate the proposed method for image segmentation and bias field estimation as follows.

3.4 Energy Formulation:

The above described local intensity clustering property indicates that the intensities in the neighbourhood φ_y can be classified in to N clusters with centers $m_i \approx b(y)C_i, i = 1, \ldots, N$, This allows us to apply the standard K-means clustering to classify these local intensities. Specifically, for the intensities$bI(X)$ in the neighbourhood φ_y , the K-means algorithm is an iterative process to minimize the clustering criterion [19], which can be written in a continuous form as

$$F_Y = \sum_{i=1}^{N} \int_{\varphi_y} I(X) - m_i^{\,2}\, u_i(X) dx \qquad (6)$$

Where m_i is the cluster center of the $i-th$ cluster, $u_i$is the mem $X \in \Omega_i$ and $u_i(X) = 0$ for $X \notin \Omega_i$. Since u_i is the membership function of the region Ω_i , we can rewrite F_y as

$$F_Y = \sum_{i=1}^{N} \int_{\Omega_i \cap \varphi_y} I(X) - m_i^{\,2} \mathrm{dx}. \qquad (7)$$

In view of the clustering criterion in (7) and the approximation of the cluster center by

$m_i \approx b(y)C_i$, we define a clustering criterion for classifying the intensities in φ_y as

$$\epsilon_Y = \sum_{i=1}^{N} \int_{\Omega_i \cap \varphi_y} K(y-x)\, I(X) - b(y)C_i^2\, dx \qquad (8)$$

Where $K(y-x)$ is introduced as a nonnegative window function, also called kernel function, such that $K(y-x) = 0$ for $X \notin \varphi_y$.With the window function, the clustering criterion function ϵ_y can be rewritten as

$$\epsilon_Y = \sum_{i=1}^{N} \int_{\Omega_i} K(y-x)\, I(X) - b(y)C_i\ ^2\, dx \quad (9)$$

This local clustering criterion function is a basic element in the formulation of our method.

3.5 Multiphase Level Set Formulation:

For the case of $N \geq 3$, we can use two or more level set functions $\emptyset_1, \ldots, \emptyset_k$ to define N membership functions m_i of the regions $\Omega_i, i = 1, \ldots, N,$, such that

$$M_i(\emptyset_1(y), \ldots, \emptyset_k(y)) = \begin{cases} 1, & y \in \Omega_i \\ 0, & else \end{cases} .$$

For example, in the case of $= 3$, we use two level set functions $\emptyset_1 \; and \; \emptyset_2$ to define

$M_1(\emptyset_1,\emptyset_2) = H(\emptyset_1)H(\emptyset_2), M_2(\emptyset_1,\emptyset_2 = H(\emptyset_1)(1-H(\emptyset_2))$

And $M_3(\emptyset_1,\emptyset_2) = 1 - H(\emptyset_1)$ to give a three-phase level set formulation of our method. For the four-phase case $N = 4$, the definition of M_i can be defined as

$M_1(\emptyset_1,\emptyset_2) = H(\emptyset_1)H(\emptyset_2), M_2(\emptyset_1,\emptyset_2) = H(\emptyset_1)\big(1 - H(\emptyset_2)\big), M_3(\emptyset_1,\emptyset_2) = \big(1 - H(\emptyset_1)\big)H(\emptyset_2),$

and $M_4(\emptyset_1,\emptyset_2) = \big(1 - H(\emptyset_1)\big)\big(1 - H(\emptyset_2)\big).$

For notational simplicity, we denote these level set functions $\emptyset_1, \dots, \emptyset_k$ by a vector valued function $= \emptyset_1, \dots, \emptyset_k$.

Thus, the membership functions $M_i(\emptyset_1(y), \dots, \emptyset_k(\emptyset))$ can be written as $M_i(\Phi)$. The energy ε in (10) can be converted to a multiphase level set formulation $\varepsilon(\Phi, c, b) = \int \sum_{i=1}^{N} e_i(X) M_i\big(\Phi(X)\big)dx$ With e_i given by (16). For the function $\Phi = (\emptyset_1, \dots, \emptyset_k)$,

This defines the regularization Terms $L(\Phi) = \sum_{j=1}^{k} L(\emptyset_j)$ and $R_p(\Phi) = \sum_{j=1}^{k} R_p(\emptyset_j)$,

Where $L(\emptyset_j)$ and $R_p(\emptyset_j)$ are defined by (19) and (20) for each level set function $\emptyset_j$, respectively. The energy functional F in our multiphase level set formulation is defined by

$$F(\Phi, b, c) \triangleq \varepsilon(\Phi, b, c) + R_p(\Phi). \qquad (25)$$

The minimization of the energy $F(\Phi, c, b)$ in (25) with respect tto the variable $\Phi = (\emptyset_1, \dots, \emptyset_k)$ can be performed by solving the following gradient flow equations:

$$\frac{\partial \emptyset_1}{\partial t} = -\sum_{i=1}^{N} \frac{\partial M_i(\emptyset)}{\partial \emptyset_1} e_i + v\partial(\emptyset_1) div\left(\frac{\nabla \emptyset_1}{|\nabla \emptyset_1|}\right)$$

$$+ \mu div((d_p(|\nabla \emptyset_1|)\nabla \emptyset_1)$$

$$\vdots$$

$$\frac{\partial \emptyset_k}{\partial t} = -\sum_{i=1}^{N} \frac{\partial M_i(\emptyset)}{\partial \emptyset_k} e_i + v\partial(\emptyset_k) div\left(\frac{\nabla \emptyset_k}{|\nabla \emptyset_k|}\right)$$

$$+ \mu div(d_p(|\nabla \emptyset_k|)\nabla \emptyset_k).$$

4. IMPLEMENTATION AND SIMULATION RESULTS:

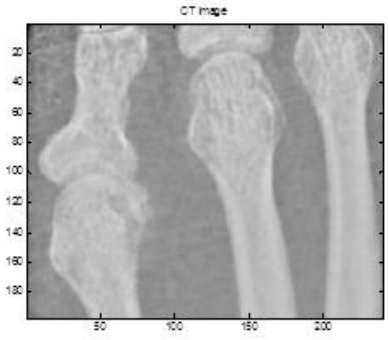

Fig 1. showsInput Of CT Image of bones

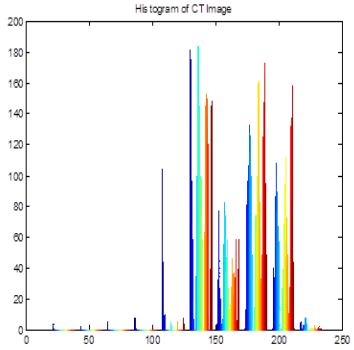

Fig 2. gives Histogram of CT Image With Density

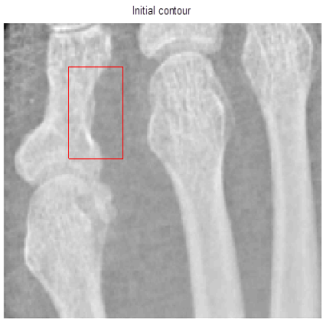

Fig 3. Iterations are Performed to the Input Image

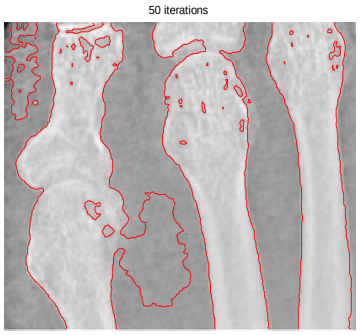

Fig 4. CT image with 50 Iterations

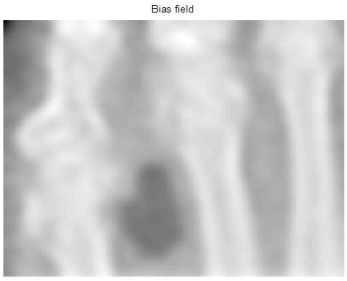

Fig 5. Blurring Of Input Image for Checking from Initial Point of the Image

Fig 6. Input Image Of Bias Corrected Image

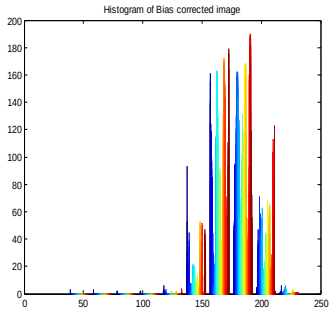

Fig 7. Image describes Histogram of Bias Corrected Image

5.Conclusion:

This work presents a variational level set framework for segmentation and bias correction of images with intensity inhomogeneities. Based on a generally accepted model of images with intensity inhomogeneities and a derived local intensity clustering property, the work defines an energy of the level set functions that represent a partition of the image domain and a bias field that accounts for the intensity inhomogeneity. Segmentation and bias field estimation are therefore jointly performed by minimizing the proposed energy functional. The slowly varying property of the bias field derived from the proposed energy is naturally ensured by the data term in our variational framework, without the need to impose an explicit smoothing term on the bias field. The proposed method is much more robust to initialization than the piecewise smooth model. Experimental results have demonstrated superior performance of our method in terms of accuracy, efficiency, and robustness.

6. ACKNOWLEDGMENTS:

The work was supported by my guide S.Asif Hussain from Annamacharya Institute of Technology & Sciences,,Rajampet ,India under Research grants of R.P.S A.I.C.T.E, New delhi.

Author Profile:

Lokeswar Reddy.Kokatam received B.Tech Degree in Electronics& Communication Engg. from JNT University, Annanthapur, India. Presently he is with Annamacharya Institute of Technology & Sciences, Rajampet, A.P., India in Dept. of ECE and pursuing his M.Tech. His research interests include Signal Processing, Time Series Analysis and Image Processing.

Asif Hussian.Shaik received B.Tech & M.Tech Degree in Electronics & Communication Engg. from JNT University, Hyderabad, India. He is currently working towards PhD Degree in Biomedical Image Processing at JNTU University, Annantapur, India. Presently he is with Annamacharya Institute of Technology & Sciences, Rajampet, A.P., India. He is working as Assistant Professor in Dept. of ECE. He presented many research papers in National & International Conferences & journals. He is a member of Professional societies like ISTE (India), BMESI (India), IACSIT (Singapore), IAENG (Hongkong) and WASE (Hongkong).His research interests include Signal Processing, Time Series Analysis and Image Processing.

7. REFERENCES

[1] Olabarriaga, S.D. and Smeulders, A.W.M., "Interactionin the Segmentation of Medical Images: A Survey",*Med. Image Analysis*, 5: 127-142, 2001.

[2] Osher, S. and Sethian, J.A., "Fronts Propagating withCurvature Dependent Speed: Algorithms Based onHamilton-Jacobi Formulations", *J. Comp. Physics*, 79:12-49, 1988.

[3] P. N. T.Wells and M. Halliwell, "Speckle in ultrasonic imaging," *Ultrasonics*,vol. 19, pp. 225–229, 1981.

[4] A. N. Evans and M. S. Nixon, "Biased motion-adaptive temporal filteringfor speckle-reduction in echocardiography," *IEEE Trans. Med.Imag.*, vol. 15, pp. 39–50, Feb. 1996.

[5] V. Caselles, R. Kimmel, and G. Sapiro, "Geodesic active contours,"*Int. J. Comput. Vis.*, vol. 22, no. 1, pp. 61–79, Feb. 1997.

[6] T. Chan and L. Vese, "Active contours without edges," *IEEE Trans.Image.Process.*, vol. 10, no. 2, pp. 266–277, Feb. 2001.

[7] S. Kichenassamy, A. Kumar, P. Olver, A. Tannenbaum, and A. Yezzi,"Gradient flows and geometric active contour models," in *Proc. 5th Int.Conf. Comput. Vis.*, 1995, pp. 810–815.

[8] R. Kimmel, A. Amir, and A. Bruckstein, "Finding shortest paths onsurfaces using level set propagation," *IEEE Trans. Pattern Anal.Mach.Intell.*, vol. 17, no. 6, pp. 635–640, Jun. 1995.

[9] C. Li, C. Kao, J. C. Gore, and Z. Ding, "Minimization of region-scalablefitting energy for image segmentation," *IEEE Trans. ImageProcess.*, vol. 17, no. 10, pp. 1940–1949, Oct. 2008.

[10] R. Malladi, J. A. Sethian, and B. C.Vemuri, "Shape modeling with frontpropagation: A level set approach," *IEEE Trans. Pattern Anal. Mach.Intell.*, vol. 17, no. 2, pp. 158–175, Feb. 1995.

[11] R. Ronfard, "Region-based strategies for active contour models," *Int.J.Comput. Vis.*, vol. 13, no. 2, pp. 229–251, Oct. 1994.
[12] C. Samson, L. Blanc-Feraud, G. Aubert, and J. Zerubia, "A variationalmodel for image classification and restoration," *IEEE Trans. PatternAnal. Mach. Intell.*, vol. 22, no. 5, pp. 460–472, May 2000.
[13] S. Theodoridis and K.Koutroumbas, *Pattern Recognition*. NewYork:Academic, 2003.
[14] A. Tsai, A. Yezzi, and A. S.Willsky, "Curve evolution implementationof the Mumford-Shah functional for image segmentation, denoising,interpolation, and magnification," *IEEE Trans. Image Process.*, vol. 10,no. 8, pp. 1169–1186, Aug. 2001.
[15] A. Vasilevskiy and K. Siddiqi, "Flux-maximizing geometric flows,"*IEEE Trans. Pattern Anal. Mach. Intell.*, vol. 24, no. 12, pp. 1565–1578,Dec. 2002.
[16] L. Vese and T. Chan, "A multiphase level set framework for imagesegmentation using the Mumford and Shah model," *Int. J. Comput. Vis.*,vol. 50, no. 3, pp. 271–293, Dec. 2002.